RSC Advances

PAPER

View Article Online
View Journal | View Issue

Cite this: *RSC Adv.*, 2024, **14**, 11124

pH-responsive niosome-based nanocarriers of antineoplastic agents†

Viliana Gugleva,[a] Rositsa Mihaylova,[b] Georgi Momekov,[b] Katya Kamenova,[c] Aleksander Forys,[d] Barbara Trzebicka,[d] Maria Petrova,[e] Iva Ugrinova,[e] Denitsa Momekova*[f] and Petar D. Petrov *[c]

Differences in pH between the tumour interstitium and healthy tissues can be used to induce conformational changes in the nanocarrier structure, thereby triggering drug release at the desired site. In the present study, novel pH-responsive nanocarriers were developed by modifying conventional niosomes with hexadecyl-poly(acrylic acid)$_n$ copolymers (HD-PAA$_n$). Niosomal vesicles were prepared by the thin film hydration method using Span 60, Span 60/Tween 60 and cholesterol as main constituents, and HD-PAA modifiers of different concentrations (0.5, 1, 2.5, 5 mol%). Next, two model substances, a water-soluble fluorescent dye (calcein) and a hydrophobic agent with pronounced antineoplastic activity (curcumin), were loaded in the aqueous core and hydrophobic membrane of the elaborated niosomes, respectively. Physicochemical properties of blank and loaded nanocarriers such as hydrodynamic diameter (D_h), size distribution, zeta potential, morphology and pH-responsiveness were investigated in detail. The cytotoxicity of niosomal curcumin was evaluated against human malignant cell lines of different origins (MJ, T-24, HUT-78), and the mechanistic aspects of proapoptotic effects were elucidated. The formulation composed of Span 60/Tween 60/cholesterol/2.5% HD-PAA$_{17}$ exhibited optimal physicochemical characteristics (D_h 302 nm; ζ potential −22.1 mV; high curcumin entrapment 83%), pH-dependent drug release and improved cytotoxic and apoptogenic activity compared to free curcumin.

Received 21st February 2024
Accepted 1st April 2024

DOI: 10.1039/d4ra01334d

rsc.li/rsc-advances

Introduction

The key advantages of nanoparticulate drug delivery systems such as small size, functionality, capacity to encapsulate wide variety of bioactive substances and thus to improve their physicochemical characteristics and bioavailability have attracted enormous research interest, leading to constant improvement and evolution of nanomedicine.[1,2] The site-specific drug delivery is especially beneficial in cancer therapeutics, as it contributes to diminished systemic toxicity, reduced side effects and enhanced therapeutic efficacy.[3,4] In particular, the elaboration of stimuli-responsive nanocarriers, which are able to release their cargo in response to specific triggers (*e.g.*, temperature, pH, redox potential, ionic composition, *etc.*) is a very promising concept for development of advanced nanocarriers.[5,6] Niosomes are nanoscale drug delivery systems possessing good biocompatibility, biodegradability, and low toxicity.[7,8] They are vesicular aggregates, identical to liposomes, but their bilayer membrane is composed of non-ionic surfactants (along with cholesterol) instead of phospholipids.[9] This fact imparts to niosomes superior chemical stability, reduced cost of production, and facilitated scale-up.[10,11] Niosomes have been exploited as feasible nanocarriers for delivery of hydrophobic and hydrophilic drugs, biologically active compounds, genetic material, as well as imaging agents in diagnostics/theranostics.[12,13] Drug delivery of natural phytochemicals has been a challenging task due to their inherent disadvantageous properties such as high molar mass, limited aqueous solubility, low chemical stability, predisposition to photodegradation.[14] In terms of topical application, these limitations may be overcome by developing advanced vesicular carriers, *e.g.*, aspasomes (ascorbyl palmitate-based vesicles),[15] bilosomes (biles salts containing vesicular systems),[16] elastic liposomes,[17,18] or ultradeformable vesicles.[19–21] The last two types of nanocarriers

[a]*Department of Pharmaceutical Technologies, Faculty of Pharmacy, Medical University of Varna "Prof. Dr Paraskev Stoyanov", 84 Tsar Osvoboditel Str., 9000 Varna, Bulgaria*
[b]*Department of Pharmacology, Pharmacotherapy and Toxicology, Faculty of Pharmacy, Medical University of Sofia, 2 Dunav Str., 1000 Sofia, Bulgaria*
[c]*Institute of Polymers, Bulgarian Academy of Sciences, bl.103 Akad. G. Bonchev Str.,1113, Sofia, Bulgaria. E-mail: ppetrov@polymer.bas.bg*
[d]*Centre of Polymer and Carbon Materials, Polish Academy of Sciences, ul. M. Curie-Skłodowskiej 34, Zabrze, Poland*
[e]*Institute of Molecular Biology "Akad. Roumen Tsanev", Bulgarian Academy of Sciences, Acad. G. Bonchev str., bl 21, Sofia 1113, Bulgaria*
[f]*Department of Pharmaceutical Technology and Biopharmaceutics, Faculty of Pharmacy, Medical University of Sofia, 2 Dunav Str., 1000 Sofia, Bulgaria. E-mail: dmomekova@pharmfac.mu-sofia.bg*

† Electronic supplementary information (ESI) available. See DOI: https://doi.org/10.1039/d4ra01334d

contain in their structure an edge activator like sodium cholate or Polysorbate 80 to impart enhanced elasticity/deformability (*vs.* the conventional liposomes) and to increase thereby drug permeation and bioavailability. In terms of systemic delivery of natural chemotherapeutics, improved therapeutic effectiveness may be obtained by modifying the vesicular structure *via* inclusion of different ligands (aptamers, receptor ligands, antibodies, *etc.*) intended to achieve target selectivity, or functional polymers for imparting stimuli-responsive properties.[22,23] For instance, elaborating polymer-modified pH-responsive niosomes, has been exploited as cancer targeting strategy as the altered microenvironment in the tumour affected tissues (mild hyperthermia, acidic pH, increased glutathione concentration), may serve as feasible and predictable indicator to utilize, in comparison to the uneven and diverse expression of target receptors in the affected areas.[24,25] The increased anaerobic glycolysis in cancer cells determines an extracellular pH ranging from 6.4 to 7.0 (*vs.* 7.2–7.4 in normal tissues), whereas the ATP-driven H^+ pump further lowers the pH in endosomes to 4.5–6.5, creating thereby a pH gradient, that allows a selective cargo release from the pH-responsive nanocarriers.[26,27] By analogy with liposomes, this process is facilitated by a pH-dependent destabilization of the niosomal membrane,[5,28] or by the fusogenic activity of the vesicles.[29] A series of pH-responsive niosomes have already been reported in the literature. In some of the formulations the stimuli responsiveness is acquired by altering the constituents, for example using cholesteryl hemisuccinate instead of cholesterol,[25,30] or by derivatizing the non-ionic surfactants, as reported by Marzoli *et al.*, which developed Tween 20-glycine based niosomes.[31] Other interesting approaches include coating the vesicles with pH (low) insertion peptide,[32] or pH-sensitive polymers. Leroux *et al.* synthesized randomly- and terminally-alkylated copolymers of *N*-isopropylacrylamide and glycine acrylamide as the pH-sensitive moiety.[28,33] The binding of copolymers to niosomes was achieved by hydrogen bonding, but the complexes formed were unstable in serum and the systems lost their pH-sensitivity. Hyaluronic acid (HA)-decorated niosomes have been developed for tacrolimus ocular delivery[34] and targeted delivery of epirubicin to breast cancer cells.[35] The authors emphasized the positive effect of modifying niosomal surface properties regarding the interaction of nanocarriers with cells (improved mucoadhesion and cell internalization as compared to the non-modified niosomes), but they did not unambiguously discuss whether the presence of pH sensitive moiety is beneficial in terms of release of the active substance.

Our research group adopted the polymer-based approach to impart pH-responsiveness of the vesicles by newly synthesized amphiphilic copolymers based on hexadecyl- and poly(acrylic acid) segments. The pH-sensitivity of the nanocarriers was demonstrated *via* the release profile of two model substances: the hydrophilic dye (calcein) and the hydrophobic drug (curcumin) as a function of pH.

Curcumin, a polyphenol extracted from the roots of *Curcuma longa*, is well-known for its antineoplastic properties.[36] The latter are attributed to a variety of complex mechanisms, including downregulation of STAT 3 (signal transducer and activator of transcription 3) and NF-κB (nuclear factor kappa B) signalling pathways, stimulation of apoptosis, as well suppression of tumour proliferation.[37,38] However, curcumin is characterized by low solubility in water, chemical and photoinstability.[39,40] Additionally, it possesses insufficient oral bioavailability, due to its low absorption and rapid biotransformation, which further favours its inclusion into nanocarriers such as niosomes.[41–44]

The present study describes the development of novel pH-responsive niosome-based carriers for delivery of active agents with potential anticancer application. Polymers comprising a lipophilic hexadecyl and a pH-sensitive poly(acrylic acid) segments were synthesized and incorporated into the niosomal aggregates, fabricated from Tween 60, Span 60, and cholesterol. The effect of polymer concentration on the structural stability of niosomes, as well as the pH-triggered release of curcumin at conditions resembling tumour cells were evaluated. Finally, comprehensive *in vitro* assays were applied to evaluate the anticancer activity and the mechanistic aspects behind it of the developed pH-responsive niosomal formulations in comparative way *vs.* free drug or loaded into plain niosomes curcumin.

Results and discussion

Synthesis of copolymers

Polymers comprising a short lipophilic hexadecyl and a pH-sensitive poly(acrylic acid) segments were synthesized by a three step procedure involving preparation of: (i) hexadecyl-based ATRP initiator, (ii) hexadecyl-poly(*t*-butyl acrylate) precursors, and (iii) hexadecyl-poly(acrylic acid) final products (Fig. 1). We aimed at obtaining polymers with an aliphatic hexadecyl (C_{16}) segment, which is compatible with the

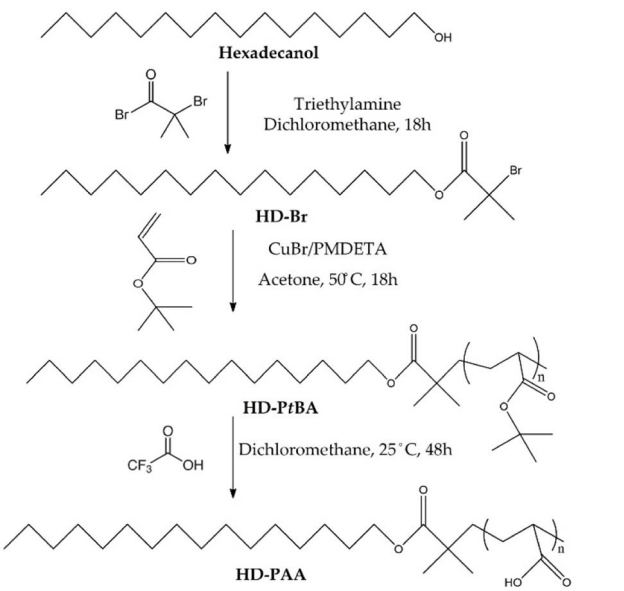

Fig. 1 Synthesis of hexadecyl-poly(acrylic acid) polymers (HD-PAA) *via* ATRP of *tert*-butyl acrylate from hexadecyl-based macroinitiator (HD-Br), and subsequent hydrolysis of the poly(*t*-butyl acrylate) blocks with trifluoroacetic acid.

constituents of the lipid bilayer of niosomes, and a PAA segment which is soluble in aqueous media at neutral pH and tends to be insoluble in acidic media, due to the protonation/deprotonation of the pendant carboxyl groups. The synthesized compounds were characterized by ^{1}H-NMR (Fig. 2) analysis and the calculated composition and number-average molar mass (M_n) are listed in Table 1. The number-average degree of polymerization of *t*BA was determined taking into account the relative intensity of integrals assigned to the methyl protons of hexadecyl chain-end (–CH_3, δ = 0.88 ppm, a) and methine protons of *t*BA main chain (–CH–, δ = 2.21 ppm, f). ^{1}H-NMR provided also direct evidence for the efficient reactions of obtaining an ATRP initiator from hexadecanol and converting P*t*BA to PAA *via* hydrolysis. In the last case, the characteristic peak of the *tert*-butyl protons at 1.45 ppm (h, Fig. 2) was not detected in the spectra of HD-PAA polymers (Fig. S1†).

GPC chromatograms of HD-P*t*BA precursors were monomodal with narrow molar mass distribution, which indicate the high efficiency of HD-Br initiator and good control over the ATRP process (Fig. 3). The number-average molar masses and dispersity indices (M_w/M_n) of the precursors, calculated from the GPC analysis are given in Table 1.

Table 1 Composition and molecular characteristics of HD-Br, HD-P*t*BA and HD-PAA

Sample code	M_n^{NMR} (g mol^{-1})	M_n^{GPC} (g mol^{-1})	M_w/M_n
HD-Br	390	510	1.01
HD-P*t*BA$_8$	1415	1850	1.10
HD-PAA$_8$	820	—	—
HD-P*t*BA$_{12}$	1930	3100	1.17
HD-PAA$_{12}$	1100	—	—
HD-P*t*BA$_{17}$	2600	3200	1.20
HD-PAA$_{17}$	1470	—	—

Preparation and characterization of pH-responsive niosomes

A series of conventional and polymer-modified niosomes based on Span 60, Span 60/Tween 60 and cholesterol were prepared by the thin film hydration method. The niosomal compositions (type of surfactants as well surfactant/cholesterol ratio) were selected based on our previous study.[45] The design of the current study was chosen following the consideration to investigate the influence of copolymers type and concentration on the physicochemical characteristics on two types of vesicles: the one exhibiting tight and rigid bilayer membrane (Sp60 : Chol 1 : 1 molar ratio) and second characterized with leakier vesicular structure, but high curcumin entrapment (Tw60 : Sp60 : Chol 3.5 : 3.5 : 3). The results from the conducted experiments are summarized in Table 2. The expected pH-induced change in membrane permeability, allowing release of the active substance, for HD-PAA$_8$-modified niosomes was not observed (see section pH-induced calcein leakage). Therefore, data related to these compositions are not described. As evident from the obtained results, copolymers type and concentration, as well as curcumin's inclusion exhibit a pronounced effect on nanocarriers' size. Blanc niosomes are characterized by larger sizes compared to drug-loaded, which may be rated to curcumin's interaction with the lipophilic region of the surfactant molecules and its accommodation in the hydrophobic membrane. The latter determines the formation of more compact structure, resulting in vesicles size reduction. Regarding copolymers inclusion, an inverse relationship was estimated between their concentration and vesicles size – a higher molar fraction of HD-PAA$_{12}$ or HD-PAA$_{17}$ leads to a decrease in niosomal diameter. The latter may be a result of the enhanced steric repulsion between the hydrophilic blocks of the copolymer, determining an increase in niosomes' curvature and, respectively a decrease in their size. Additionally, the incorporated in the niosomal membrane hydrophobic block of the copolymer may interact with the molecules of non-ionic surfactants and cholesterol, which increases the integrity of the niosomal membrane. Polymer content also affected the size distribution pattern of the vesicles – the higher the molar ratio of HD-PAA$_{12}$ and HD-PAA$_{17}$ the higher the polydispersity index. A possible explanation for such behavior may be the reaching

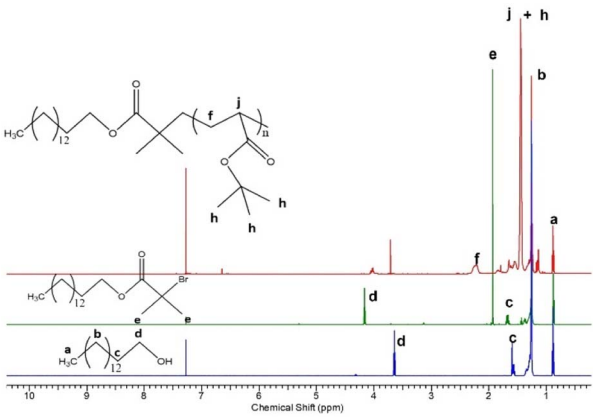

Fig. 2 ^{1}H-NMR spectra of hexadecanol (bottom), hexadecyl-based ATRP initiator (middle), and hexadecyl-poly(*t*-butyl acrylate)$_{12}$ precursor (top) in $CDCl_3$.

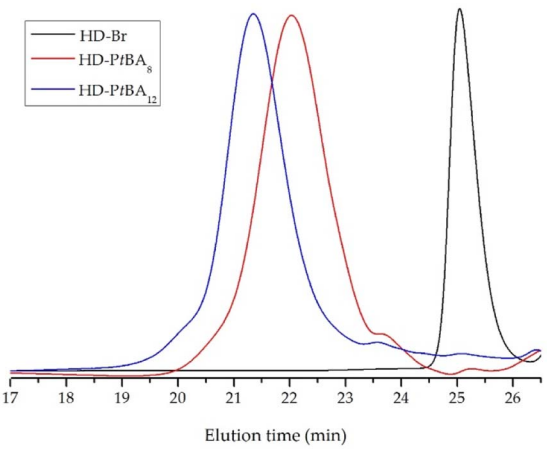

Fig. 3 GPC chromatograms of HD-Br, HD-P*t*BA$_8$ and HD-P*t*BA$_{12}$ with THF as the eluent.

Table 2 Composition, physicochemical characteristics, and entrapment efficacy of curcumin-loaded niosomes, prepared by TFH method

Sample	SF : Chol (mol : mol)	HD-PAA$_{12}$ (mol%)	HD-PAA$_{17}$ (mol%)	D_h (nm)	PDI	ζ-Potential (mV)	EE (%)	DL (%)
S1	Sp60 : Chol (1 : 1) (blank)	—	—	573 ± 5.2	0.45 ± 0.03	−8.7 ± 0.4	—	—
S2	Sp60 : Chol (1 : 1)	—	—	389 ± 5.2	0.31 ± 0.02	−5.7 ± 0.4	27 ± 1.6	1.23
S3	Tw60 : Sp60 : Chol (3.5 : 3.5 : 3) (blank)	—	—	489 ± 4.8	0.34 ± 0.06	−12.3 ± 2.3	—	—
S4	Tw60 : Sp60 : Chol (3.5 : 3.5 : 3)	—	—	379 ± 3.3	0.32 ± 0.02	−12.2 ± 2.1	80 ± 1.8	2.03
S5	Sp60 : Chol ((1 : 1)	0.5	—	464 ± 4.2	0.27 ± 0.04	−17.7 ± 0.7	28 ± 1.6	1.28
S6	Sp60 : Chol (1 : 1)	1	—	478 ± 5.9	0.31 ± 0.02	−20.2 ± 1.4	29 ± 1.6	1.33
S7	Sp60 : Chol (1 : 1)	2.5	—	330 ± 4.2	0.25 ± 0.05	−21.2 ± 1.1	32 ± 1.6	1.47
S8	Sp60 : Chol (1 : 1)	5	—	237 ± 8.4	0.5 ± 0.02	−23.9 ± 2.5	21 ± 1.6	0.96
S9	Tw60 : Sp60 : Chol (3.5 : 3.5 : 3)	0.5	—	293 ± 5.5	0.37 ± 0.02	−19.2 ± 1.8	81 ± 0.9	2.06
S10	Tw60 : Sp60 : Chol (3.5 : 3.5 : 3)	1	—	391 ± 5.9	0.41 ± 0.06	−21.7 ± 0.6	80 ± 2.8	2.04
S11	Tw60 : Sp60 : Chol (3.5 : 3.5 : 3)	2.5		324 ± 3.3	0.38 ± 0.03	−22.1 ± 1.4	83 ± 1.3	2.12
S12	Tw60 : Sp60 : Chol (3.5 : 3.5 : 3)	5	—	332 ± 8.1	0.55 ± 0.06	−24.8 ± 1.3	71 ± 1.8	1.81
S13	Sp60 : Chol (1 : 1)	—	0.5	602 ± 3.3	0.38 ± 0.06	−21.3 ± 0.7	29 ± 2.8	1.33
S14	Sp60 : Chol (1 : 1)	—	1	654 ± 7.5	0.4 ± 0.01	−22.5 ± 1.1	30 ± 1.1	1.38
S15	Sp60 : Chol (1 : 1)	—	2.5	563 ± 4.6	0.36 ± 0.04	−23.8 ± 1.2	30 ± 3.4	1.38
S16	Sp60 : Chol (1 : 1)	—	5	519 ± 5.8	0.48 ± 0.05	−23.1 ± 0.9	28 ± 2.5	1.28
S17	Tw60 : Sp60 : Chol (3.5 : 3.5 : 3)	—	0.5	324 ± 9.5	0.32 ± 0.04	−20.4 ± 0.4	81 ± 1.8	2.06
S18	Tw60 : Sp60 : Chol (3.5 : 3.5 : 3)	—	1	363 ± 6.7	0.42 ± 0.07	−24.3 ± 1.5	80 ± 3.4	2.04
S19	Tw60 : Sp60 : Chol (3.5 : 3.5 : 3)	—	2.5	302 ± 6.6	0.34 ± 0.02	−21.1 ± 1.7	83 ± 2.8	2.12
S20	Tw60 : Sp60 : Chol (3.5 : 3.5 : 3)	—	5	299 ± 9.5	0.45 ± 0.03	−23.5 ± 0.8	76 ± 2.2	1.94

and exceeding of the saturation limit of membranes with respect to investigated polymers, which leads to a subsequent destabilizing effect onto niosomal integrity, respectively disruption of the lamellar structure and formation of transient structures – discs or micelles. Zeta potential also increased with the inclusion of higher molar fraction of modifying copolymers. The obtained high negative values are a prerequisite for optimal colloidal stability of niosomal dispersions due to the electrostatic repulsion between the vesicles, preventing their aggregation (Table 2). Regarding the entrapment efficiency values, no significant changes in curcumin encapsulation were observed within the concentration range (0.5–2.5 mol%) for both studied polymers. However, in the formulations based on HD-PAA$_{12}$ the increase of copolymer concentration above 2.5 mol% (S8 and S12) was accompanied by more than 10% decrease in curcumin entrapment efficiency, which was probably due to the competitive interactions between the plain counterparts are very small to claim a beneficial effect of the membrane modification of niosomes on the solubilization and entrapment of curcumin. Based on the obtained results, it can be concluded that the optimal concentration of modifying copolymer for the elaboration of curcumin loaded niosomes was 2.5 mol%. This conclusion was also confirmed by the microscopic evaluation of the structure of elaborated vesicles. Representative micrographs of conventional and copolymer modified niosomes are depicted in Fig. 4. All formulated vesicles exhibited spherical shape with a smooth surface. As evident from the presented data, the inclusion of the pH-sensitive copolymers in a concentration of up to 2.5 mol% doesn't disrupt the unilamellar vesicular structure and copolymer molecules and the hydrophobic curcumin. In the formulations modified with HD-PAA$_{17}$ the tendency was preserved, however in a less pronounced manner. A similar trend is observed also in regard of drug loading capacity. Despite the observed slight increase in the curcumin loading with the increase of the mole fraction of copolymers (up to 2.5 mol%), the differences in the loading capacity of the modified vesicles compared to their integrity of niosomes. However, at 5 mol%, a concomitant small fraction of discs and micelles was observed (Fig. S2†).

pH-induced calcein leakage

An integral part of the detailed characterization of modified niosomes was the evaluation of their pH-responsiveness. For this purpose, a series of calcein-loaded niosomes, modified with

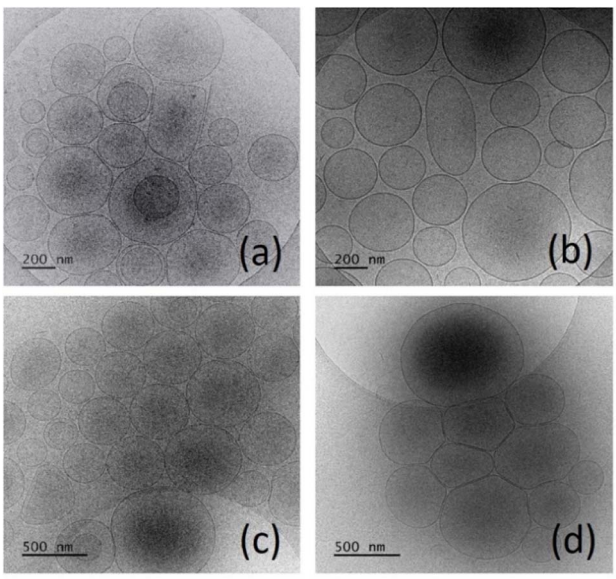

Fig. 4 Cryo-TEM images of niosomes: (a) Sp60 : Chol, (b) Tw60 : Sp60 : Chol; (c) Sp60 : Chol : HD-PAA$_{12}$ (2.5 mol%), (d) Tw60 : Sp60 : Chol : HD-PAA$_{12}$ (2.5 mol%).

HD-PAA$_{12}$ and HD-PAA$_{17}$ were prepared. Calcein is a water-soluble, polar compound, which fluorescence at concentration of 80 mM is self-quenched and is not dependent on variations in pH. The polar nature of calcein limits its passage through intact niosomal membranes. However, when the membrane is disrupted as result of changes in the pH of the medium, calcein will be released. Consequently, its concentration decreases due to dilution in the release medium, leading to an increase in the fluorescence of the dye. The results of the spectrofluorometric study of niosomes as a function of pH are illustrated in Fig. 5. As evident from the obtained results, the inclusion of studied copolymers into niosomal membranes leads to pH-triggered destabilization of the niosomal membranes. Thus, a pH-induced release of more than 70% of the encapsulated fluorescent dye was achieved only after 10 minutes of incubation in a slightly acidic media. At the same time, calcein release from modified niosomes after 24 h incubation in PBS pH 7.4 at 37 °C exhibited lower release rate compared to non-modified vesicles (Fig. 6). To elucidate the mechanism of the observed pH-dependent calcein release profile, we performed a comparative DLS analysis of HD-PAA$_{17}$ modified niosomes before and after 10 min incubation at 37 °C in isotonic media with pH 7.4 and 5.5, respectively. While at the initial moment there is no difference in the size and size distribution between the vesicles at pH 7.4 and 5.5, after 10 minutes of incubation at 37 °C, a decrease by about 10% of size of niosomes in the acidic medium, as well as a slight increase in PDI compared to vesicles at pH 7.4 was clearly observed (Fig S3†). This is probably due to changes in the lamellar organization of the bilayers, in response to conformational changes of PAA moieties upon their protonation in the acidic environment.

Usually, upon gradual decrease in pH the polyanion chains undergo a collapse from an expanded coil-like conformation to a contracted, globule-like conformation. This is due to the protonation of the carboxylic groups, which makes the polymer more hydrophobic. In the case of polyanion-modified vesicles, at a certain point the deprotonated polymer becomes membrane active, *i.e.*, it leads to an increased lateral compression of the bilayer and disruption of the membrane.[46] The pH at which this happens is dependent on the hydrophilic/hydrophobic balance of the modifying molecules. Philippova

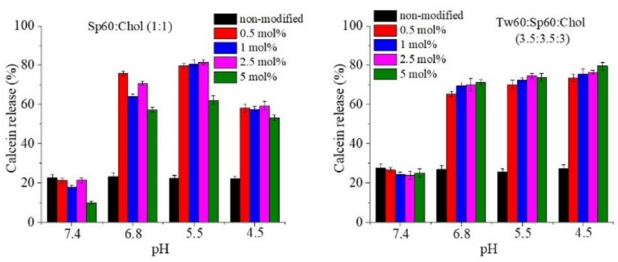

Fig. 5 pH-dependent calcein release from HD-PAA modified niosomes after 10 min incubation at 37 °C in PBS pH 7.4/6.8/5.5/4.5. The selected pH values are representative for the pH in tumor interstitium (pH 7–6.8); early endosomes (pH 6.5); late endosomes (pH 5.5) and lysosomes (pH 4.5).

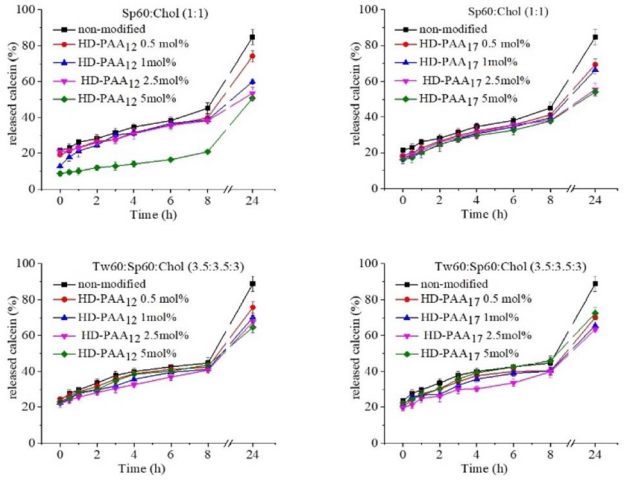

Fig. 6 Calcein release in PBS pH 7.4 at 37 °C as a function of copolymer concentration.

et al. reported that the addition of hydrophobic alkyl residue to the poly(acrylic acid) backbone shifts the transition to a higher value as compare to the pure PAA.[47] In addition, hydrogen bonding between the polyanion molecules and the vesicle surface also contributes to the shift of the coil-to-globule transition to higher pH values.[46] The results from calcein leakage experiments undoubtedly demonstrate the potential of the elaborated pH-responsive niosomes to serve as effective platform for targeted drug delivery and pH-triggered release of water-soluble drugs in pathologically altered tissues (*e.g.*, in tumour interstitium, or in specific subcellular compartments, characterized with lower pH values than physiological), while simultaneously preserve their stability and integrity in systemic circulation environment. A subsequent stage in our study was to evaluate curcumin release from copolymer modified niosomes in dissolution media with different pH values. As all copolymer modified vesicles exhibited pH-responsive properties, the *in vitro* release studies were conducted with the formulation characterized with the smallest size and highest curcumin entrapment efficiency – Sp60 : Tw60 : Chol : HD-PAA$_{17}$ (S19).

In vitro release of curcumin from optimal niosomal formulation

The release profile of curcumin from HD-PAA$_{17}$ modified niosomes was investigated as a function of pH for 24 hours (Fig. 7a). Curcumin exhibited a pH-dependent release pattern inversely proportional to the corresponding pH values. The highest release rate was estimated at pH 5.5, with approximately 1.6 and 1.5-fold increased cumulative drug release compared to those at pH 7.4 and pH 7.4 + 10% albumin. A possible explanation may lie in the pH-dependent ionization of polyelectrolytes. At neutral or alkaline conditions, PAA is deprotonated, which contributes to its good solubility and swelling in aqueous medium. In an acidic environment, on the contrary, PAA is prone to protonation, which leads to diminished solubility, dissociation[48] and ultimately determines the

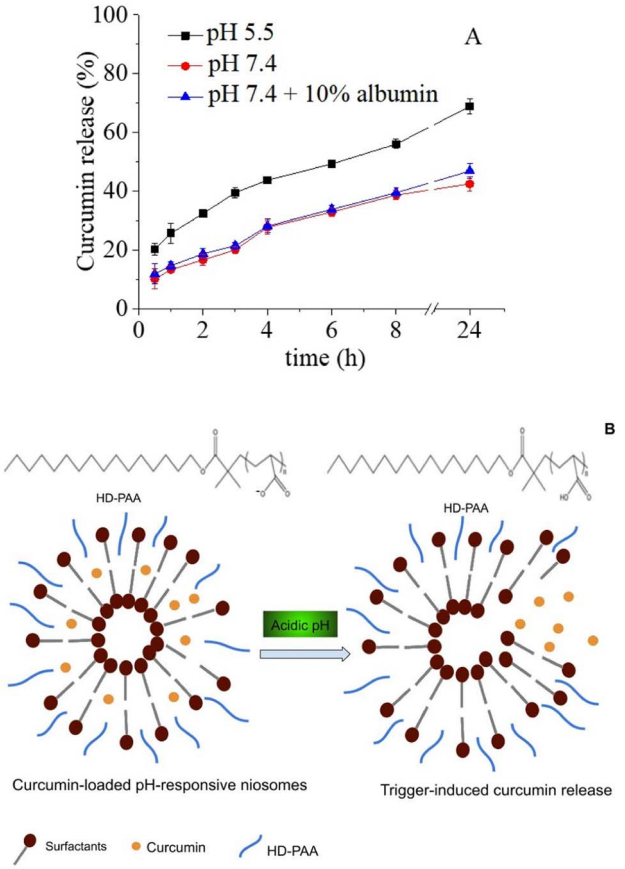

Fig. 7 Curcumin cumulative release from HD-PAA$_{17}$ modified niosomes based on Sp60 : Tw60 : Chol as a function of pH and time (A) and schematic presentation of membrane rearrangements at acid pH (B).

higher release of encapsulated curcumin. A schematic illustration of the process is shown on Fig. 7b. Similar tendency in the drug release pattern was reported also by Saroj and Rajput, which elaborated poly(acrylic acid)-modified mesoporous silica nanoparticles.[49] The included albumin in the release medium (PBS, pH 7.4) determined the slightly higher curcumin release compared to plain PBS. The latter may be due to the absorption of albumin onto niosomal surface, which may result into a transient void in their structure, leading to increased membrane permeability. Similar findings were reported by Hioki *et al.*, which investigated doxorubicin release from conventional and PEGylated liposomes.[50] This high retention of curcumin in niosomes at pH 7.4 is a precondition for improved chemical stability of the drug in the circulation and is also essential for the aptitude of the carrier to deliver the cargo to the desired tissue or cell compartment at optimal concentration.

As the elaborated systems are designed as potential parenteral preparations, following systemic administration the tissue distribution is expected to occur within several hours and at such stage the pH-sensitive properties would condition beneficial behavior in tissues and compartments with lower pH, incl. tumor interstitium and subcellulary inside endosomes, long before the first 24 h.

Stability of niosomes

The stability is one of the main requirements for niosomes as drug carriers. In other words, they have to maintain their key physicochemical characteristics and the amount of the encapsulated drug unchanged for a certain period of time. In this regard, the stability of selected niosomal compositions was monitored for a period of one month when stored in a refrigerator at a temperature of 4 °C. The data on the main parameters of the vesicles immediately after their preparation and one month later are presented in Table 3. The results obtained demonstrated that both plain and polymer modified niosomal formulations are stable upon storage at low temperature for at least one month as there is no evidence for deterioration of the main parameters of niosomes: size, PDI and encapsulation efficacy of curcumin. This can be due to the presence of cholesterol and modifying copolymer in niosomal membranes, which in combination with low temperature of storage hampers the molecular movements of membrane constituents and thus, preventing the merging of niosomes.

Cellular internalization of niosomes

Habitually, the cellular internalization of nanocarriers involves a near contact between cell and niosomal membranes. As the PAA segments of the copolymers used in this study are deprotonated at physiological environment (pH 7.4), this fact determines the negative zeta potential of the developed HD-PAA modified niosomes (Table 2). Although the influence of the ζ-potential on the *in vivo* behavior of niosomes is complex, and the effects described in the literature are not unambiguous, there are many data proving that the presence of a negative zeta-potential favors the cellular internalization of the vesicles.[51] On this ground it was worthy to investigate whether the presence of hydrophilic PAA layer on the niosomal surface could affect their ability to interact with target cells. Thus, *in vitro* cellular uptake of curcumin by H1299 and L929 (data not shown) cells, treaded with subequieffective concentrations of free or niosomal curcumin encapsulated into plain Tw60 : Sp60 : Chol niosomes (S4) or into their HD-PAA$_{12}$ or HD-PAA$_{17}$ modified counterparts (S11, S19) was studied by fluorescence microscopy. The tested cell lines H1299 and L929 were selected as models of sensitive adherent malignant and nonmalignant cells. As shown in Fig. 8 A and B, H1299 cells treated with the niosomal curcumin showed greater green fluorescence intensity than those treated with the free drug. Presumably, the encapsulated curcumin in niosomes penetrates the cell by endocytosis, which is the predominantly mechanism of internalization of nanosized carriers and is much more effective than the simple diffusion of free drug.[52] The encapsulation into the niosomes increased its accumulation in the cells, which is evident from the bar graph representing the quantification of the normalized integrated density. In the case of plain niosomes, an increase of 60% was observed, while polymer-modified niosomes showed approximately 2.6-fold higher fluorescence intensity as compared to the free curcumin (Fig. 8B). Normally, after internalization in the cells, curcumin accumulates partially on endoplasmic membranes, clathrin vesicles, and lysosomes.[53] Such

Table 3 Physical stability evaluation of selected plain and copolymer modified curcumin niosomes

Sample	Time (days)	D_h (nm)	PDI	ζ-Potential (mV)	EE (%)
Tw60 : Sp60 : Ch (S4)	0	379 ± 3.3	0.32 ± 0.02	−12.2 ± 2.1	80 ± 2
	30	382 ± 4.2	0.35 ± 0.01	−11.5 ± 1.8	79 ± 2
Tw60 : Sp60 : Ch : HD-PAA_{17} (S19)	0	302 ± 6.6	0.34 ± 0.01	−21.1 ± 1.7	83 ± 3
	30	298 ± 2.4	0.34 ± 0.03	−22.6 ± 2.1	83 ± 2

localization was observed for the free and niosomal curcumin encapsulated into the HD-PAA_{12} modified niosomes. Interestingly, HD-PAA_{17} modified vesicles, which contains a more extended PAA component, shows colocalization of curcumin with the nuclear-specific marker DAPI (Fig. 8C and arrows in panel A), demonstrating the ability of the engineered vesicles to overcome lysosomal retention and deliver cargo to target subcellular compartments. The observed effective targeting of the nucleus was not a primary consideration in our formulation design strategy, but it is a noteworthy discovery.

Cytotoxicity assessment of free and niosomal curcumin

MTT – assay. To evaluate whether the encapsulation of curcumin into the elaborated pH-sensitive niosomes would result into an augmentation of its antineoplastic activity, we investigated the cytotoxic potential of niosomal curcumin in comparative way *vs.* the free drug. The experiments were performed with niosomes of different surfactant compositions modified with 2.5 mol% of the two HD-PAA pH-responsive copolymers due to their excellent physicochemical and release characteristics. The cytotoxic activity of curcumin-loaded niosomes was studied against human malignant cell lines of different origins (MJ, T-24, HUT-78). The experimental data obtained were normalized as percentages of the untreated control and processed mathematically by nonlinear regression analysis using the GraphPad Prism software. Based on this, "dose–response" relationships were derived (Fig. 9) and the half-inhibitory concentrations (IC_{50}) were calculated (Table 4). All experimental niosomal formulations exerted a dose-dependent cytotoxicity varying in degree in a cell-line specific

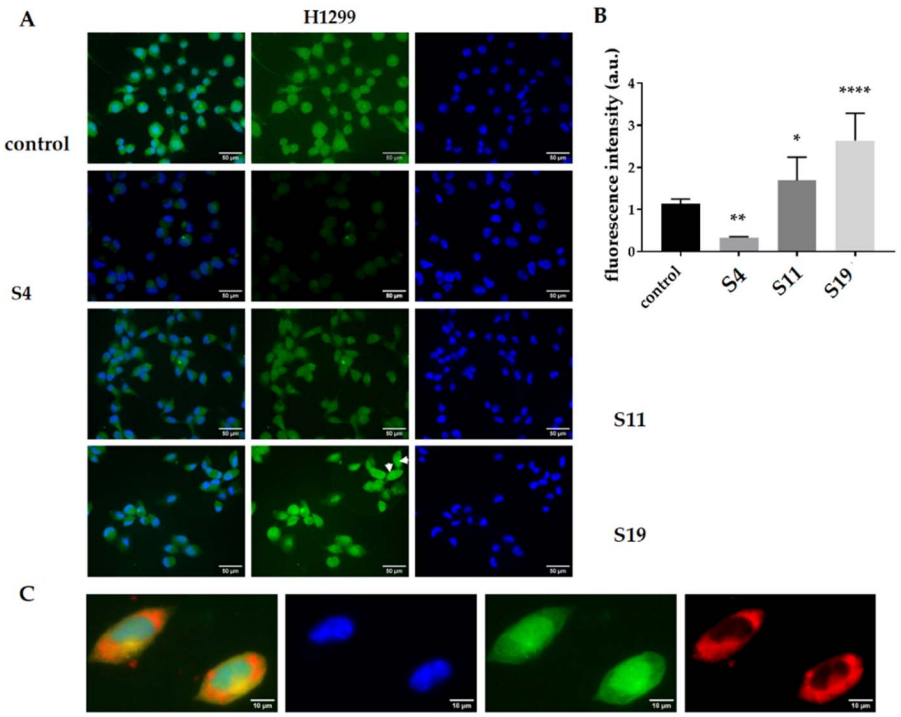

Fig. 8 (A) Representative microscopic images of cellular uptake of H1299 cells treated for 6 hours with pure curcumin (first line), non-modified niosomes (second line) formulation S4, drug encapsulated in S11 niosomes (third line), and drug encapsulated in S19 niosomes (fourth line). The natural fluorescence of curcumin is green, and nuclear contra staining with DAPI is blue. Arrows indicated cells with nuclear localization of curcumin-loaded T-17 niosomes. (B) Quantification of normalized integrated density in A.U. The integrated density was measured by Fiji quantification tool. For each condition, at least five images were measured. Multiple comparisons function of One-way ANOVA (Dunnett's multiple comparison test) was used to compare the mean of niosomes-treated cells with the mean of the control column of pure curcumin-treated cells. Probability values were considered significant at the *$p < 0.05$, **$p < 0.01$, and ****$p < 0.0001$. (C) Representative microscopic images showing the accumulation of curcumin encapsulated in T-17 niosomes in the nucleus of some cells. The natural fluorescence of curcumin is green, the cell membrane is stained with CellMask Orange in red, and nuclear contra staining with DAPI is blue.

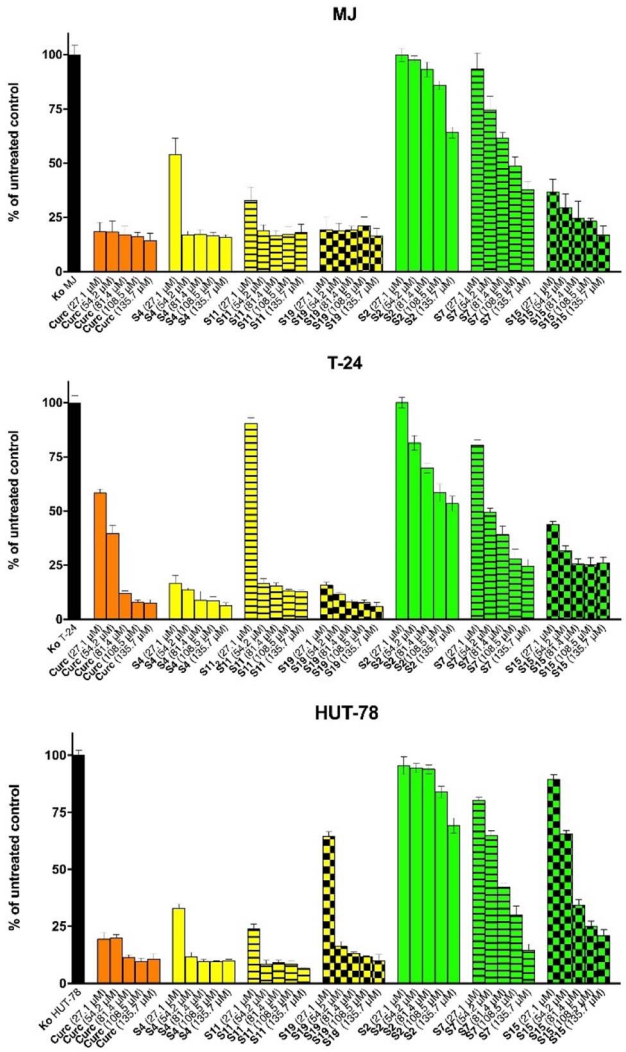

Fig. 9 Cytotoxic effect of free and loaded curcumin in conventional and pH-sensitive niosomes against a panel of human malignant cell lines determined by a MTT-dye reduction assay after 72 h continuous exposure. SD represents the mean values of 8 independent experiments.

manner. A clear pattern in the cellular effects of the niosomal carriers was also observed depending on their composition and structure. The highest antitumor activity with IC_{50} values in the low micromolar concentration range exhibited the HD-PAA_{17}-modified pH-sensitive niosomes based on Tw60 : Sp60 : Chol, equivalent (in the MJ cell line) and nearly seven times exceeding (in the T-24 malignant culture) the cytotoxicity of the reference substance curcumin. The alternative HD-PAA_{12}-modified niosomal formulation (S11) demonstrated a slightly lower antiproliferative potential, however, still matching the activity of the reference free drug in the other screened T-cell lymphoma model (HUT-78). Satisfactory results were also obtained with the unmodified variant of curcumin-loaded Tw60 : Sp60 : Chol niosomes, which inhibited T-24 cells' growth nearly seven times more effectively than the reference substance (IC_{50} 5.5 μM *vs.* 34.9 μM, respectively). The least favourable cytotoxicity profile showed plain Sp60 : Chol niosomes and its stimuli-responsive counterparts modified with HD-PAA_{12} (S7) in all of the screened malignant cell lines.

Clonogenic assay. The antiproliferative effects of the most potent curcumin loaded niosomal formulation Tw60 : Sp60 : Ch : HD-PAA_{17} were further assessed in a comparative way *vs.* free agent or loaded into plain niosomes curcumin by using clonogenic assay in H1299 cancer cells after 48 h exposure to their equieffective levels. The clonogenic assay is a valuable tool for assessing the fraction of cells that retain their proliferative ability and form colonies after exposure to a cytotoxic agent. We treated H1299 cells with calculated IC_{50} values (see ESI, Table S1 and Fig. S4†) of free curcumin, loaded in plain niosomes curcumin (S4), and their HD-PAA_{17} modified counterparts (S19) for 48 hours at two different cell concentrations (500 and 1000 cells per well). Then the cells were allowed to grow for 10 days in drug-free medium. Curcumin has demonstrated potential anticancer effects, including inhibition of cancer stem cells and induction of senescence and clonogenic death in breast cancer cells.[54] We sought to determine whether curcumin loaded in pH-sensitive niosomes retained the cytotoxic capacity of the free drug. Our results revealed that although there are no statistically significant differences in the survival fractions of H1299 cells treated with either free curcumin or niosomal curcumin (Fig. 10) the less colonies were count in cells treated with HD-PAA-modified systems. These findings suggest that curcumin-loaded pH-sensitive niosomes could serve as a promising drug delivery system for cancer treatment. Encapsulation of the drug in niosomes may enhance its effectiveness and minimize potential side effects. However, further investigation is necessary to explore the full potential of this approach and its clinical applications.

Table 4 Equieffective concentrations (IC_{50}) of free curcumin and its niosomal formulations. IC_{50} (μM ± SD) in terms of curcumin concentration

IC_{50} (μM ± SD) in terms of curcumin concentration			
Sample/cell line	MJ	T-24	HUT-78
Curc	3.3 ± 1.2	34.9 ± 2.8	6.4 ± 1.8
Tw60 : Sp60 : Ch (S4)	26.4 ± 2.3	5.5 ± 1.7	14.2 ± 2.4
Tw60 : Sp60 : Ch : HD-PAA_{12} (S11)	18.2 ± 3.4	41.2 ± 4.3	8.7 ± 1.7
Tw60 : Sp60 : Ch : HD-PAA_{17} (S19)	2.3 ± 1.1	5.2 ± 1.5	33.0 ± 2.5
Sp60 : Ch (S2)	140.2 ± 8.3	142.9 ± 7.6	154.8 ± 9.5
Sp60 : Ch : HD-PAA_{12} (S7)	101.8 ± 10.4	59.7 ± 3.6	67.5 ± 4.4
Sp60 : Ch : HD-PAA_{17} (S15)	10.39 ± 2.1	18.7 ± 3.1	67.6 ± 3.2

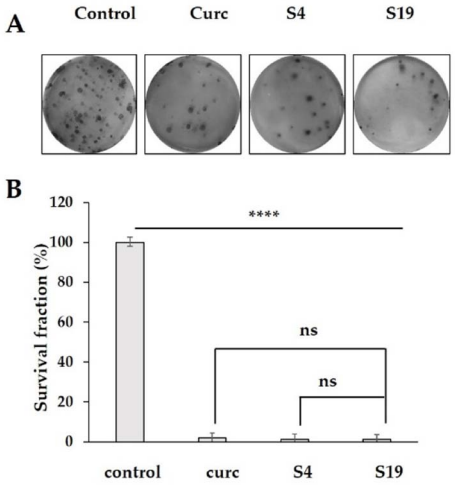

Fig. 10 Clonogenic assay of untreated H1299 cells (control) or cells treated with IC_{50} concentrations of curcumin loaded pH-sensitive Tw60 : Sp60 : Ch : HD-PAA_{17} niosomes (S19), curcumin-loaded plain niosomes (Tw60 : Sp60 : Ch) (S4) and pure curcumin. (A) A photograph of a representative experiment is shown. Graph quantifications of colony number (B). The mean values of two independent experiments performed in duplicates are presented with standard deviation ($n = 2$) ±SD. One-way ANOVA Tukey's multiple comparisons test was used to tests each experimental group against each control group. Probability values are ****$p < 0.001$.

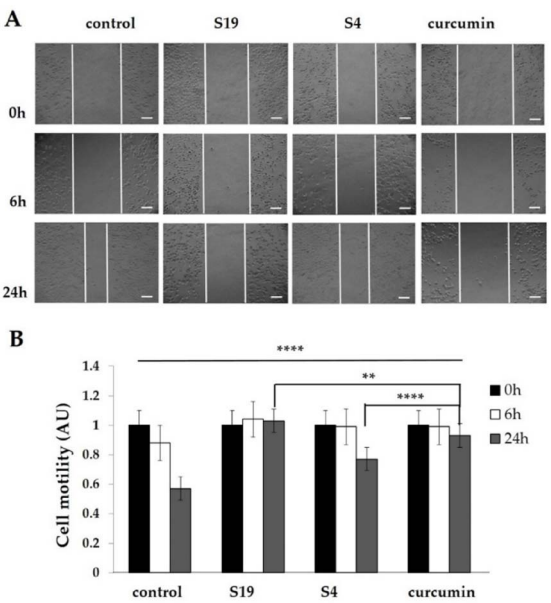

Fig. 11 Wound healing scratch assay of H1299 cells. (A) Wound closure over 24 hours for H1299 cells treated with IC_{50} concentrations of curcumin loaded pH-sensitive Tw60 : Sp60 : Ch : HD-PAA_{17} niosomes (S19), curcumin-loaded plain niosomes (Tw60 : Sp60 : Ch) (S4) and pure curcumin. Scale bar corresponds to 100 μM. (B) Bar graph presenting quantitative analyzes of wound closure. Results are representative of three independent experiments and displayed as mean + SEM for duplicate wells. ** = $p < 0.01$; **** = $p < 0.001$; statistical comparison of area was determined by ANOVA Tukey's multiple comparisons test.

Scratch assay (wound-healing assay). Recent research studies have reported that curcumin exhibits an inhibitory effect on cell migration and invasion of various cancer cell lines. This process of cell migration is essential for the movement of cells from one location to another and is involved in critical processes such as wound healing, immune response, and cancer metastasis.[55] Curcumin can exert its effect on cell migration *via* multiple mechanisms such as modulation of protein expression, signaling pathways, and miRNA expression.[56] One of the tools used to study the effect of drugs on cell migration ability is the scratch assay, which enables the investigation of the inhibitory effect of curcumin on cell relocation *in vitro*. In this line, we sought to determine the efficacy of curcumin loaded in pH-sensitive niosomes to constrain cell migration of H1299 cells *in vitro* in comparative way *vs.* free or loaded into plain niosomes agent by using the scratch assay. Specifically, H1299 cells were grown to near 80% confluence, wounds were introduced, and the cells were treated for 24 hours with IC_{50} concentrations of free drug or its pH-sensitive or plain niosomal formulations. The cells were then photographed at the 0, 6th and 24th hour (Fig. 11A). Our results revealed that encapsulated in pH-sensitive niosomes curcumin significantly reduced the migration of H1299 cells compared to the control group (Fig. 11B, $p < 0.001$). The same trend is observed also for the free drug. In contrast, curcumin loaded in the non-modified niosomes (S4) showed only a moderate effect. These results suggest that curcumin has a potent inhibitory effect on cell migration and the loading of curcumin in pH-sensitive HD-PAA_{17} – modified vesicles can further enhance its efficacy. To delineate whether the observed antiproliferative activity of the elaborated curcumin-loaded niosomal formulations was due to modulation of the cytotoxic potential of curcumin and not to the carriers themselves we sought out to evaluate the cytotoxic potential of non-loaded vesicles as well as of HD-PAA copolymers. As seen from the results depicted on Fig. S4† the tested formulations are devoid of cytotoxicity, as the inhibition in cell proliferation was not higher that 20% as compared to the untreated control. According to the presented results, the encapsulation of curcumin into niosomal delivery systems has a modulatory effect on their spectrum of antitumor activity, possibly due to changes in their release kinetics, induced by the modifying HD-PAA_{12} and HD-PAA_{17} polymers. Some of the investigational compositions (S19) emerge as promising drug delivery carriers with a great potential for further scientific development.

Proteomic analysis. Based on the curcumin effects on cellular and humoral immune functions, we sought to determine the therapeutic relevance of different curcumin formulations for potential local application in cutaneous T cell lymphoma and bladder carcinoma malignancies, whether as transdermal therapeutic systems or intravesical instillations. The biological and pharmacological evaluation of the curcumin-loaded niosomal systems was approached in two perspectives: investigation of the molecular basis of their cytotoxicity (Fig. 12 and 13) and studying their potential effects on inflammation (Fig. 14 and 15) in bladder carcinoma (T-24) and

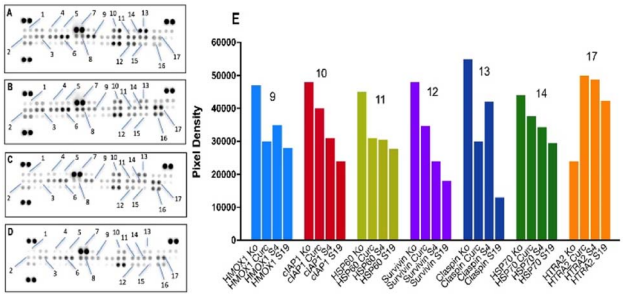

Fig. 12 Changes in expression levels of apoptosis-related proteins in T-24 cells following treatment with: curcumin (B); Tw60 : Sp60 : Chol – S4 (C); Tw60 : Sp60 : Chol : HD-PAA$_{17}$ – S19 (D), as compared to untreated control (A). Cells were exposed to equieffective concentrations (IC$_{50}$) of free curcumin and its niosome formulations for 24 h, following which a human proteome profiler assay was performed according to manufacturer's instructions. Further densitometric analysis of the array spots was conducted using ImageJ software and the most prominent changes in the proteome were ex-pressed graphically (E). Legend: 1 – bad; 2 – TRAILR1, 3 – TRAILR2; 4 – bcl-2; 5 – bcl-*x*; 6 – fas, CD95; 7 – pro-caspase 3; 8 – HIF-1α; 9 – HMOX1 (anti-apoptotic); 10 – cIAP1; 11 – HSP60; 12 – survivin; 13 – claspin; 14 – HSP70; 15 – TNF RI; 16 – XIAP; 17 – HTRA/Omi.

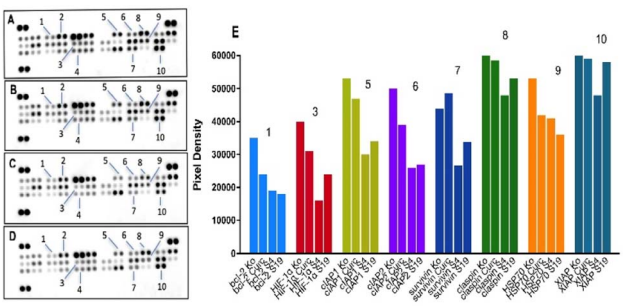

Fig. 13 Changes in expression levels of apoptosis-related proteins in MJ cells following treatment with: curcumin (B); Tw60 : Sp60 : Chol – S4 (C); Tw60 : Sp60 : Ch : HD-PAA$_{17}$ – S19 (D), as compared to untreated control (A). Cells were exposed to equieffective concentrations (IC$_{50}$) of free curcumin and its niosome formulations for 24 h, following which a human proteome profiler assay was performed according to manufacturer's instructions. Further densitometric analysis of the array spots was conducted using ImageJ software and the most prominent changes in the proteome were ex-pressed graphically (E). Legend: 1 – bcl-2; 2 – bcl-*x*; 3 – HIF-1α; 4 – phospho p53; 5 – cIAP1; 6 – cIAP2; 7 – survivin; 8 – claspin; 9 – HSP70; 10 – XIAP.

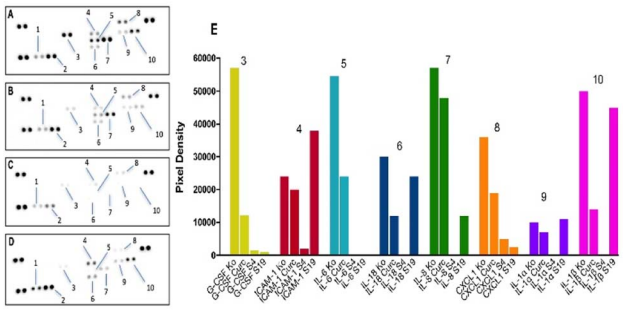

Fig. 14 Changes in expression levels of inflammation-related proteins in T-24 cells following treatment with: curcumin (B); Tw60 : Sp60 : Chol – S4 (C); Tw60 : Sp60 : Ch : HD-PAA$_{17}$ – S19 (D), as compared to untreated control (A). Cells were exposed to equieffective concentrations (IC$_{50}$) of free curcumin and its niosome formulations for 24 h, following which a human cytokine profiler assay was performed according to manufacturer instructions. Further densitometric analysis of the array spots was conducted using ImageJ software and the most prominent changes in the proteome were expressed graphically (E). Legend: 1 – MIF; 2 – PAI1; 3 – G-CSF; 4 – ICAM-1; 5 – IL-6; 6 – IL-18; 7 – IL-8; 8 – CXCL1; 9 – IL-1α; 10 – IL-1β.

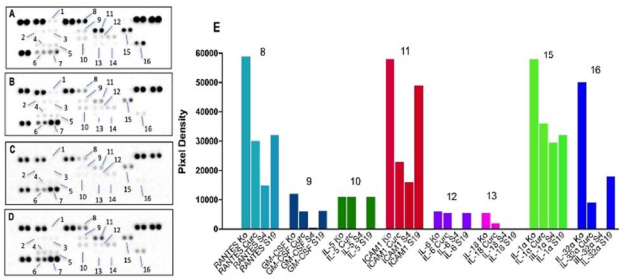

Fig. 15 Changes in expression levels of inflammation-related proteins in MJ cells following treatment with: curcumin (B); Tw60 : Sp60 : Ch – S4 (C); Tw60 : Sp60 : Ch : PAA$_{17}$ – S19 (D), as compared to untreated control (A). Cells were exposed to equieffective concentrations (IC$_{50}$) of free curcumin and its niosome formulations for 24 h, following which a human cytokine profiler assay was performed according to manufacturer instructions. Further densitometric analysis of the array spots was conducted using ImageJ software and the most prominent changes in the proteome were expressed graphically (E). Legend: 1 – CCL2/MCP-1; 2 – CXCL11/I-TAC; 3 – CXCL12/SDF-1; 4 – IL-13; 5 – IL-16; 6 – MIF; 7 – SERPIN E1/PAI-1; 8 – CCL5/RANTES; 9 – GM-CSF; 10 – IL-5; 11 – ICAM1/CD54; 12 – IL-6; 13 – IL-18; 14 – IL-21; 15 – IL-1α; 16 – IL-32α.

cutaneous T cell lymphoma (MJ) *in vitro* models using curcumin as a reference drug. The parallel determination of multiple apoptosis-related proteins revealed particular changes in the expression profiles of several molecular end-points in both tumor models.

As indicated by the proteomic data for T-24 cells (Fig. 12), both curcumin and its niosomal formulations failed to evoke cleavage of the procaspase 3 zymogen (7), that acts as a central executor caspase in the final stages of the apoptotic cascade. Changes in the activity of the bcl-2 cell death regulators bad (1, proapoptotic), bcl-2 and bcl-*x* (antiapoptotic, 2 and 3, respectively) were also minor (Fig. 12 A–D).

Nevertheless, distinguishable changes in spot signals were registered for a number of survival factors that inhibit apoptosis at an earlier stage, including cIAP (10), survivin (12) and the chaperons HSP60, HSP70 (11 and 14, respectively). The expression profiles of these proteins follow a repetitive pattern where the strongest down-regulation (*ca.* 50% in cIAP1 and survivin levels) was induced by the HD-PAA$_{17}$-modified niosomes (S19) followed by the plain composition (S4) and the free curcumin. A similar trend with a slightly better performance of curcumin shared the proteomic imprints of HMOX1 (9) and claspin (13), although the strongest proapoptotic stimuli was invariably induced by the modified with HD-PAA$_{17}$ niosomal

variant. On the contrary, the proapoptotic serine protease HTRA/Omi that is released from mitochondria in response to cellular stress was significantly up-regulated in the treated samples regardless of curcumin formulation and slightly decreased in the following order: curcumin > plain niosomes > HD-PAA_{17}-modified niosomes (Fig. 12E).

Comparative analysis of the apoptotic response in CTCL cells (Fig. 13) also showed consistent reduction in the expression of the aforementioned survival factors cIAP1 (5), cIAP2 (6), survivin (7) and XIAP (10). However, the strongest inhibition of these factors was achieved by the plain niosomal formulation (S4) leading to a nearly 2-fold weakening in the signals for (5), (6) and (7) and a modest decline in (10). Unlike bladder carcinoma T-24 cell line, the proapoptotic activity of curcumin formulations against MJ cells followed a different trend. The most prominent changes in protein expression across all samples were induced by the unmodified niosomes, followed by its HD-PAA_{17}-modified variant and free curcumin (Fig. 13E). A slightly better performance of the pH-sensitive system was only observed in the chaperone HSP70 (9) expression profile. The two niosomal compositions yielded a decent 50% decrease of the major bcl-2 family member (1) that was less influenced by the free curcumin formulation. The found predominant modulation of early regulatory factors of cell cycle and the lack of capacity to initiate core components of the apoptotic machinery (*i.e.* procaspase 3) in curcumin and niosome samples may be a time-dependent phenomenon since protein expression was measured only 24 hours following treatment.

Human cytokine array. Interesting findings were also obtained on the inflammatory status of treated T-24 and MJ cells as compared to the control (Fig. 14 and 15). A 24 h exposure of bladder carcinoma cells (Fig. 12) to unformulated curcumin and its niosomal forms resulted in a drastic decrease in the expression levels of a panel of proinflammatory mediators, including IL-6 (5), IL-18 (6), IL-8 (7), IL-1α (9), IL-1β (10), growth factors G-CSF, (3) and adhesion molecules ICAM-1, (4). Furthermore, cytokine and chemokine suppression had a characteristic profile, dependent on curcumin composition. Thereby, both curcumin-loaded niosome carriers triggered a markedly stronger anti-inflammatory response as compared to the referent drug and superior activity was achieved by the polymer-free niosomal variant, as indicated by the complete disappearance of the spot signals for IL-6 (5), IL-18 (6), IL-8 (7), IL-1α (9), IL-1β (10) (Fig. 14A–E). Highly consistent with these findings appeared to be the immunological changes in the treated MJ cells (Fig. 15), where curcumin formulations exhibited the same order of potency: plain niosomes > HD-PAA_{17}-modified niosomes > free curcumin. Albeit weakly expressed in the control CTCL group, a complete depletion of the GM-CSF (9), IL-5 (10), Il-6 (12) and IL-18 (13) was observed in response to 24 hours exposure to Tw60 : Sp60 : Chol (S4). An absolute inhibition was also reached in IL-32 expression (16), which was initially high in the control group and plays a major role in cancer-induced chronic inflammation. The same formulation induced substantial reduction in the chemotactic RANTES protein (8) and its downstream target – the intercellular adhesion molecule 1 (ICAM-1, 11). Both mediators have been recognized as major triggers in skin inflammation that is a characteristic trait of the CTCL lesions. According to the presented data from the conducted pharmacodynamic study, both types of niosome formulations exerted an augmenting effect on curcumin performance in either of the investigated mechanistic aspects. The strongest proapoptotic stimuli in bladder carcinoma T-24 cells exerted the pH-responsive Tw60 : Sp60 : HD-PAA_{17} niosomes, whereas plain Tw60 : Sp60 : Chol vesicles had a more pronounced effect in the CTC lymphoma cells. In terms of inflammation, prevalent inhibitory effect evoked the polymer-free Tw60 : Sp60 : Chol formulation in both screened cell lines.

Experimental

Materials

Hexadecanol, α-bromoisobutyryl bromide, triethylamine, *tert*-butyl acrylate (tBA), Na_2CO_3, $MgSO_4$ Cu(I)Br, *N*,*N*′,*N*″,*N*‴-pentamethyldiethylenetriamine (PMDETA), and trifluoroacetic acid (TFA) were purchased from Sigma-Aldrich (FOT, Bulgaria) and used as received. Dichloromethane (DCM), acetone, methanol, 1,4-dioxane and tetrahydrofuran (THF) were obtained from Fisher Chemical (Labimex, Bulgaria) and distilled prior use. Curcumin (Curc), Span 60, Tween 60 and cholesterol were provided by Sigma-Aldrich (FOT, Bulgaria). Chloroform, methanol and other solvents were of analytical grade.

Methods

Synthesis of hexadecyl-based ATRP initiator. Hexadecanol (5 g, 20.6 mmol) was dissolved in dry freshly distilled dichloromethane (50 mL) in a single-neck round-bottom flask. Then, triethylamine (5.16 mL, 37 mmol, 1.8 eq.) was added to the reaction mixture *via* syringe. The solution was cooled down to 0 °C and α-bromoisobutyryl bromide (4.58 g, 37 mmol, 1.8 eq.) was added dropwise. The reaction was carried out for 18 hours at room temperature. Thereafter, the reaction mixture was filtered off to remove the white precipitate of ammonium bromide. The solution was washed 3 times with a 5 wt% Na_2CO_3. The organic phase was dried over $MgSO_4$, filtered and treated with activated carbon to remove impurities. Next, the solvent was removed by rotary evaporation and the obtained as a brown oil ATRP initiator (HD-Br) was dissolved in 1,4-dioxane and lyophilized. Yield = 65%; reaction efficiency (>99%, determined by ^{1}H-NMR); ^{1}H-NMR ($CDCl_3$, δ ppm): 4.17 (m, 2H, CH_2–C$\underline{H}_2$–O), 1.68 (m, 2H, –CH_2–C$\underline{H}_2$–CH_2–O–), 1.93 (s, 6H, –C–C$\underline{H}_3$), 1.26 (m, 26H, –CH_2–C$\underline{H}_2$–CH_2–), 0.88 (m, 3H, CH_2–C$\underline{H}_3$).

Synthesis of hexadecyl-poly(*t*-butyl acrylate). A 250 mL single-neck round-bottom flask fitted with a stir bar was charged with HD-Br (0.7 g, 1 eq.), Cu(I)Br (0.34 g, 1.5 eq.) and freshly distilled acetone (2 mL). After that, the flask was rapidly sealed off with a septum, and the reaction mixture was stirred at ambient temperature under argon flow for 20 minutes. After degassing with argon, deoxygenated PMDETA (0.5 mL, 1.5 eq.) was added *via* syringe, and the solution was allowed to stir additional 20 min to form the copper complex under argon atmosphere. Finally, deoxygenated *t*BA (10, 15 or 20 eq.) was

added, the flask was placed in an oil bath thermostated at 50 °C and the polymerization was conducted for 18 h. The resulting polymer was dissolved in THF and then the solution was passed through a silica column to remove the copper catalyst. The obtained polymer solution was concentrated and precipitated into methanol/water (70 : 30) at 4 °C. Finally, the polymer was recovered by freeze drying. Yield 76%. ^{1}H-NMR ($CDCl_3$, δ ppm): 4.17 (m, 2H, CH_2–C$\underline{H}_2$–O), 1.68 (m, 2H, –CH_2–C$\underline{H}_2$–CH_2–O–), 1.93 (s, 6H, –C–C$\underline{H}_3$), 1.26 (m, 26H, –CH_2–C$\underline{H}_2$–CH_2–), 0.88 (m, 3H, CH_2–C$\underline{H}_3$); *t*BA protons: 2.21 (s, H, –CH_2–C(C=O)$\underline{H}$–), 1.53 (m, 2H, –C$\underline{H}_2$–C(C=O)H–), and 1.45 (m, 9H, O–C(C$\underline{H}_3$)$_3$).

Synthesis of hexadecyl-poly(acrylic acid). HD-P*t*BA (1 g) was dissolved in freshly distilled dichloromethane (30 mL) in a 100 mL round-bottom flask fitted with a stir bar. After that, trifluoroacetic acid (3.7 mL; 5.0 equivalents to the *tert*-butyl groups) was added. The mixture was allowed to stir at room temperature for 48 h. Dichloromethane and the excess of TFA were removed at room temperature by purging with argon. The resulting glassy, light-brown polymer solid was vacuum-dried for 2 days. For further purification, the polymer was dissolved in 10 mL of THF/water (80 : 20) mixture, transferred into dialysis tube (3500 MWCO), and dialyzed against deionized water for 3 days. Finally, HDPAA was recovered by freeze drying.

Co-polymers characterization. ^{1}H-NMR spectra were recorded using a Bruker Avance II + 600 spectrometer at room temperature. The samples were dissolved in $CDCl_3$ or D_2O. Gel permeation chromatography (GPC) measurements were performed with a Shimadzu Nexera HPLC chromatograph equipped with a degasser, a pump, an autosampler, a RI detector and three PSS SDV columns (5 μm Linear M; 5 μm, 100 Å; and 5 μm, 50 Å), using tetrahydrofuran as the eluent at a flow rate of 1.0 mL min^{-1} and temperature 40 °C. The sample concentration was 1 mg mL^{-1} and the instrument was calibrated with polystyrene standards.

Preparation of pH-sensitive curcumin loaded niosomes. Conventional and copolymer modified curcumin niosomes were prepared applying the thin film hydration (TFH) method.[57] Non-ionic surfactants (Span 60, Span 60 : Tween 60) and cholesterol (1 : 1 and 3.5 : 3.5 : 3 molar ratio, total lipid content 30 μmoL ml^{-1}) and curcumin (1.5 μmol mL^{-1}) were dissolved in 10 mL chloroform. For the preparation of polymer modified niosomes 0.5, 1, 2.5 and 5 mol% HD-PAA_{12} or HD-PAA_{17} were dissolved in chloroform : methanol mixture (2 : 1 v/v) and added to the niosomal constituents. The organic solvents were evaporated at 60 °C using a rotary evaporator (Buchi, Germany) (150 rpm), resulting into a dried lipid film on the interior of the flask. Next, the lipid film was subsequently hydrated for 1 hour at 60 °C (100 rpm) with 10 mL PBS (pH 7.4, composition: NaCl 8.0 g L^{-1}, KCl 0.2 g L^{-1}, Na_2HPO_4 1.44 g L^{-1} and KH_2PO_4 0.245 g L^{-1}). Afterwards niosomal dispersions were sonicated for 2 min using probe sonicator (Bandelin). The elaborated curcumin-loaded niosomes were stored at 4 ± 2 °C for further evaluation.

Encapsulation efficiency. The non-entrapped curcumin was separated from niosomes by gel filtration through a Sephadex G50 column (Pharmacia, Uppsala, Sweden), equilibrated with the same hydration medium. Curcumin's content in niosomal dispersions was determined by liquid/liquid extraction. Briefly, curcumin-loaded niosomes were lysed in a chloroform/methanol mixture (1 : 1 wt/wt). Afterwards aliquots of phosphate buffered saline (pH 7.4) were added and the resultant mixture were vortexed for 10 s and centrifuged for 5 min at 6000 rpm. Curcumin's concentration in the organic layer was evaluated spectrophotometrically at 427 nm, using a UV-VIS spectrophotometer (Shimadzu UV-1800). The entrapment efficiency (EE%) and drug loading capacity (DL%) were calculated using the following equations:

$$\text{EE (\%)} = \frac{\text{amount of entrapped curc}}{\text{total amount of curc}} \times 100 \quad (1)$$

$$\text{DL (\%)} = \frac{\text{amount of entrapped curc}}{\text{total lipid}} \times 100 \quad (2)$$

The experiments were carried out three times and the average values were used.

Vesicle size, size distribution and zeta potential evaluation. The mean size, polydispersity index (PDI) and zeta potential of blank and curcumin loaded niosomes (conventional and copolymer modified) were investigated by Zetasizer NanoZs (Malvern Instruments, UK), equipped with a 633 nm laser. Niosomal formulations were measured at scattering angle of 175° at 25 °C. Vesicles size was expressed as hydrodynamic diameter (D_h). The experiment was performed in triplicate and the results are presented as mean values ± SD.

Cryogenic transmission electron microscopy (cryo-TEM). The morphology of conventional and copolymer modified curcumin niosomes was evaluated by cryogenic transmission electron microscopy. A drop of niosomal dispersion (3 μL) was applied onto a copper grid, absorbing the excess with filter paper and frozen in liquid ethane. The samples were analysed at −178 °C, using Tecnai F20 X TWIN microscope (FEI Company, Hillsboro, OR, USA), operating at an acceleration voltage of 200 kV. The images were captured by Gatan Rio 16 CMOS 4k camera (Gatan Inc., Pleasanton, CA, USA) and analysed *via* Gatan Microscopy Suite software (Gatan Inc., Pleasanton, CA, USA).

Leakage assays. Calcein-loaded niosomes were prepared by TFH method following the protocol for conventional and pH-sensitive niosomes with the difference that as hydration medium was used calcein aqueous solution at concentration 80 mM, at which its fluorescence is self-quenched. The non-entrapped dye was removed by gel-filtration through a Sephadex G50 column equilibrated with saline. 100 μL of calcein loaded niosomes were added to 2 mL of isotonic buffered solutions with pH values within the diapason 4.5 and 7.4, as follows: PBS (pH 7.4, composition: NaCl 8.0 g L^{-1}, KCl 0.2 g L^{-1}, Na_2HPO_4 1.44 g L^{-1} and KH_2PO_4 0.245 g L^{-1}); isotonic buffered solution pH 6.8 (composition: NaCl 4.06 g L^{-1}, Na_2HPO_4 5.53 g L^{-1} and KH_2PO_4 4.85 g L^{-1}); isotonic buffered solution pH 5.5 (composition: NaCl 2.77 g L^{-1}, Na_2HPO_4 1.3 g L^{-1} and KH_2PO_4 13.1 g L^{-1}) and isotonic acetate buffer pH 4.5 (composition: $C_2H_3NaO_2$ 2.99 g L^{-1}, gl. CH_3COOH 1.66 mL and NaCl 5.99 g L^{-1}). As the polar dye leaks out from niosomal membranes, it gets diluted in the release medium leading to an increase in the fluorescence. After 10 minutes of incubation at 37 °C calcein

fluorescence was evaluated at $\lambda_{emm} = 520$ nm and $\lambda_{ex} = 490$ nm, prior and after the disruption of niosomes by 100 μL of 10% v/v TritonX100 using a Hitachi 7000 spectrofluorimeter equipped with thermostatic circulating water bath. The percentage of calcein leakage was calculated applying the formula:

$$\text{Leakage } (\%) = \frac{(I_{pH} - I_{7.4})}{(I_t - I_{7.4})} \times 100 \quad (3)$$

where, I_{pH} represents the corrected intensity at acidic pH before disruption of vesicles, as $I_{7.4}$ is denoted the fluorescence at pH 7.4 and I_t represents the total fluorescence intensity assessed after lysis of niosomes.

***In vitro* curcumin release studies.** Curcumin cumulative release from developed pH sensitive niosomes was evaluated as a function of pH by dialysis method.[58] 2 mL of tested formulations were inserted into a dialysis bag (MWCO 12 000–14 000, Sigma-Aldrich, Steinheim, Germany) and placed in a 100 mL dissolution medium – phosphate-buffered saline (PBS) pH 5.5, PBS pH 7.4 and PBS pH 7.4 + 10% albumin. To all acceptor media 10% ethanol was added to maintain the solubility of the released curcumin. The acceptor medium was in constant motion (200 rpm) and the circulating water jacket (Huber, Germany) maintained the temperature at 37 ± 0.5 °C during the study. At predetermined time points 1 mL samples from the released medium were withdrawn and analyzed for curcumin by UV-VIS spectroscopy at 427 nm. The aliquots were replaced with equal volume fresh medium. The drug release studies were carried out threefold.

Stability studies. Stability of curcumin loaded plain and pH-sensitive HD-PAA_{17} modified niosomes was evaluated after one month storage at temperature 4–8 °C in refrigerator. Samples were taken at predetermined time intervals (at time 0 and after 1 month) and size, PDI, zeta-potential and curcumin entrapment efficacy were evaluated to determine the stability of the formulations.

Cell lines and culture conditions. The *in vitro* anti proliferative activity of the curcumin-loaded niosomal formulations and free curcumin was assessed in a panel of tumor cell lines of different origin namely urinary bladder carcinoma (T-24), and cutaneous T-cell lymphoma (HUT-78 and MJ). All cell lines were purchased from the German Collection of Microorganisms and Cell Cultures (DSMZ GmbH, Braunschweig, Germany). H1299 (human lung carcinoma cell line) and L929 – mouse fibroblast (from the ATCC collection of cell cultures) was purchased from LGC Limited, Augsburg, Germany and were used for evaluation of cellular internalization of the prepared niosomes. T-24, HUT-78 and MJ were cultivated in a growth medium RPMI 1640 supplemented with 10% fetal bovine serum (FBS), 5% L-glutamine, while H1299 and L929 cell were grown in RPMI-1640 and Eagle's Minimum Essential Medium, respectively, supplemented with 10% heat-inactivated fetal bovine serum, 100 units/mL penicillin, and 100 μg mL^{-1} streptomycin (Thermo Fisher Scientific, *via* Antisel Bulgaria Ltd, Sofia, Bulgaria). All cells were incubated under standard conditions of 37 °C and 5% humidified CO_2 atmosphere. All cell growth media are recommended to be adjusted to the ideal pH of 7.4 in appropriate buffer conditions to promote optimal cell proliferation. Only cells growing in the exponential phase were used.

Proteome Profiler Human Apoptosis Array Kit, R&D Systems and a Proteome Profiler Human Cytokine Array Kit, R&D Systems were used for the parallel determination of multiple apoptosis- and inflammation-related protein endpoints.

***In vitro* MTT colorimetric assay.** The *in vitro* cytotoxicity of the newly developed niosomal curcumin formulations was evaluated using a validated methodology for assessing cell viability known as the Mosmann MTT method. Exponential-phased cells were harvested and seeded (100 μL per well) in 96-well plates at the appropriate density (3×10^5 for the suspension cultures and 1.5×10^5 for the adherent T-24 cells). Following a 24 h incubation, cells were treated with five different doses of the nanocarriers in respect to curcumin concentration (135.7; 108.5; 81.4; 54.2 and 27.1 μM). After exposure time of 72 h, filter sterilized MTT substrate solution (5 mg mL^{-1} in PBS) was added to each well of the culture plate. A further 1–4 h incubation allowed for the formation of purple insoluble formazan crystals. The latter were dissolved in isopropyl alcohol solution containing 5% formic acid prior to absorbance measurement at 550 nm. Collected absorbance values were blanked against MTT- and isopropanol solution and normalized to the mean value of untreated control (100% cell viability).

Proteomic analysis. A series of immunoassay experiments were performed to monitor changes in the proteome profile of cells treated with the experimental curcumin formulations. Changes in the apoptotic and survival signaling, as well as in the inflammatory status of T-24 and MJ cells in response to 24 h exposition to free curcumin and its niosomal formulations were tracked. Membrane-based sandwich immunoassays were conducted according to manufacturer's instructions (Proteome Profiler Human Apoptosis Array Kit, R&D Systems; Proteome Profiler Human Cytokine Array Kit, R&D Systems). The arrays were visualized using a digital imaging system (Azure Biosystems C600) and densitometric analysis of the array spots was conducted using ImageJ software. The most prominent changes in the proteome were expressed graphically relative to untreated control and interpreted in a comparative manner to unformulated curcumin as a reference compound.

Statistical methods. The obtained experimental data were processed mathematically by nonlinear regression analysis using the GraphPad Prism software. Based on this, "dose–response" relationships were derived, and the half-inhibitory concentrations (IC_{50}) were calculated.

Immunofluorescence microscopy. To observe the curcumin accumulation in the treated cells, they were grown on coverslips and treated with free or loaded in the niosomal systems curcumin at a final concentration of 25 μg mL^{-1} for 6 hours. After incubation in some wells, 1× CellMask Orange (Thermo Fisher Scientific, *via* Antisel Bulgaria Ltd, Sofia, Bulgaria) was added for 15 minutes to visualize the cell membrane. The coverslips were fixed with 3.7% (v/v) paraformaldehyde in PBS for 5 min at RT and washed 3 times in 1× PBS for 5 minutes. Finally, the coverslips were mounted in ProLong Diamond mounting media containing 400 ng mL^{-1} DAPI for nucleus staining. Images were

acquired in a Zeiss AxioImager Z2 microscope using an EC Plan-Neofluar objective, 40×/0.75 Ph 2 M27, equipped with a CCD camera Axiocam 705 mono. Exposure time and detector gains were maintained at the same level during all imaging sessions. Image processing and calculations have been done using the Fiji image processing package.

Statistical analysis. Microscopic data were collected from two independent experiments. Between 5 and 10 images were analyzed for each sample. Data were analyzed using Microsoft Excel and GraphPad Prism v. 8.0 (Dotmatics, San Diego, CA, USA) and are shown as mean ± SD. A statistically significant difference was considered at $p < 0.05$ using ANOVA Dunnett's multiple comparison test.

Clonogenic assay (colony formation assay). To assess cell survival and proliferation based on the ability of a single cell to form a colony we performed a clonogenic assay. For this purpose, the cells from H1299 cancer cell line were seeded in a 6-well flat-bottomed plates (Corning Costar Flat Bottom Cell Culture Plate) at 400 single (without clumps) cells per well. The cells were treated after 24 hours of incubation at 37 °C and 5% CO_2 with IC_{50} values of free curcumin or loaded into plain and HD-PAA_{17} modified Tw60 : Sp60 : Ch niosomes for 48 hours. After incubation the medium was replaced with fresh one and the cells were allowed to grow for 10 days. Then the cells were washed 2 times for 5 min with 1× PBS. After that the cells were fixated with 4% PFA (paraformaldehyde) for 20 min at gentle shaking. After the fixation the cells were washed with 1× PBS for 5 min and stained with 0.2% Crystal-violet (Sigma-Aldrich) for 20 min at gentle shaking and room temperature. The last step was washing the cells 3 times for 5 min with dH_2O and dried at room temperature. Then the colonies were counted on ImageJ software and plating efficiency (PE) and survival fraction (SF) were calculated. Photoshop software was used for image processing. Statistical analysis was performed on GraphPad Prism v. 8.0 (Dotmatics, San Diego, CA, USA) and One-way ANOVA Tukey's multiple comparisons test was used.

Scratch assay (wound-healing assay). Scratch assay was applied to quantify cellular migration over certain time intervals on 2-dimensional (2-D) surfaces after treatment. To evaluate the cell migration, we seeded 1×10^5 H1299 cells in 12-well flat-bottomed plates (Corning Costar Flat Bottom Cell Culture Plate). After a 24 hours incubation the cells were grown to 80% confluency, a scratch was made with a 10 μL pipette tip to create an incision-like gap and the cells were treated with IC_{50} values of free and loaded curcumin in non-modified Tw60 : Sp60 : Chol and pH-sensitive HD-PAA_{17} vesicles. Images of the formed "wounded" area were taken immediately (0 hours) on Zeiss AxioVert 200M microscope using a 5× objective lens, equipped with a CCD camera Axio Cam MRm. Additional images were taken 6 and 24 hours after treatment. The length of the scratch for every time interval was measured using the Carl Zeiss™ AxioVision Rel. version 4.8 software (Fisher Scientific, Waltham, MA, USA). The cell migration at every tested condition was quantified and processed on GraphPad Prism v. 8.0 (Dotmatics, San Diego, CA, USA).

Conclusions

Original pH-responsive nanocarriers for delivery of bioactive agents were successfully elaborated by membrane modification of conventional niosomes with newly synthesized hexadecyl-poly(acrylic acid) copolymers (HD-PAA_{12} and HD-PAA_{17}). All copolymer modified niosomes exhibited pH-dependent release of the encapsulated cargo (a water soluble and a hydrophobic model drug), with higher release rate in acidic media, which may be exploited as a feasible targeting approach in cancer therapeutics. The formulation composed of Span60 : Tween60 : cholesterol : HD-PAA_{17} (2.5 mol%) were characterized by small size (302 nm), high curcumin entrapment efficiency (83%) and increased cellular internalization. In addition, the curcumin-loaded pH-responsive niosomes showed a higher inhibition on colony formation and enhanced antineoplastic and anti-inflammatory activity compared to free drug. Furthermore, the results from the conducted pharmacodynamic study revealed the strongest proapoptotic stimuli in bladder carcinoma T-24 cells for the optimal Span60 : Tween60 : cholesterol : HD-PAA_{17} formulation. Therefore, the elaborated pH-responsive niosomes may be explored as a feasible platform for targeting delivery of curcumin.

Author contributions

Denitsa Momekova: conceptualization, formal analysis, investigation, writing—original draft preparation, writing – review and editing, funding acquisition. Petar D. Petrov: conceptualization, formal analysis, investigation, writing – sections, writing – review and editing. Georgi Momekov: formal analysis, investigation, writing – review and editing. Iva Ugrinova: formal analysis, investigation, writing – sections, writing – review and editing. Viliana Gugleva: investigation, writing – original draft preparation, writing – sections, review, and editing. Rositsa Mihaylova: investigation, writing – sections, review, and editing. Katya Kamenova: investigation, writing – sections. Aleksander Forys: investigation, writing – sections. Barbara Trzebicka: writing – sections, review, and editing. Maria Petrova: investigation, writing – sections.

Conflicts of interest

There are no conflicts to declare.

Acknowledgements

This work was supported by the Bulgarian National Science Fund (grant КП-06-43/3-2020). P. P. and B. T. acknowledge the scientific cooperation between the Bulgarian Academy of Sciences and the Polish Academy of Sciences (project IC-PL/12/2024-2025).

Notes and references

1 S. A. A. Rizvi and A. M. Saleh, Applications of nanoparticle systems in drug delivery technology, *Saudi Pharm. J.*, 2018, **26**(1), 64–70.
2 O. Afzal, A. S. A. Altamimi, M. S. Nadeem, S. I. Alzarea, W. H. Almalki, A. Tariq, B. Mubeen, B. N. Murtaza,

S. Iftikhar, N. Riaz and I. Kazmi, Nanoparticles in drug delivery: from history to therapeutic applications, *Nanomaterials*, 2022, **12**(24), 4494.

3 Y. Yao, Y. Zhou, L. Liu, Y. Xu, Q. Chen, Y. Wang, S. Wu, Y. Deng, J. Zhang and A. Shao, Nanoparticle-based drug delivery in cancer therapy and its role in overcoming drug resistance, *Front. Mol. Biosci.*, 2020, **7**, 193.

4 D. Mundekkad and W. C. Cho, Nanoparticles in clinical translation for cancer therapy, *Int. J. Mol. Sci.*, 2022, **23**(3), 1685.

5 S. Saraf, A. Jain, A. Tiwari, A. Verma, P. K. Panda and S. K. Jain, Advances in liposomal drug delivery to cancer: An overview, *J. Drug Delivery Sci. Technol.*, 2020, **56**, 101549.

6 N. M. AlSawaftah, N. S. Awad, W. G. Pitt and G. A. Husseini, pH-Responsive nanocarriers in cancer therapy, *Polymers*, 2022, **14**(5), 936.

7 D. G. Bhavani and V. L. Lakshmi, Recent advances of non-ionic surfactant-based nano-vesicles (niosomes and proniosomes): a brief review of these in enhancing transdermal delivery of drug, *Futur. J. Pharm. Sci.*, 2020, **6**, 100.

8 B. A. Witika, K. E. Bassey, P. H. Demana, X. Siwe-Noundou and M. S. Poka, Current advances in specialised niosomal drug delivery: manufacture, characterization and drug delivery applications, *Int. J. Mol. Sci.*, 2022, **23**(17), 9668.

9 M. Masjedi and T. Montahaei, An illustrated review on nonionic surfactant vesicles (niosomes) as an approach in modern drug delivery: Fabrication, characterization, pharmaceutical, and cosmetic applications, *J. Drug Delivery Sci. Technol.*, 2021, **61**, 102234.

10 X. Ge, M. Wei, S. He and W. E. Yuan, Advances of non-ionic surfactant vesicles (niosomes) and their application in drug delivery, *Pharmaceutics*, 2019, **11**(2), 55.

11 S. Grijalvo, G. Puras, J. Zárate, M. Sainz-Ramos, N. A. L. Qtaish, T. López, M. Mashal, N. Attia, D. Díaz Díaz, R. Pons, E. Fernández, J. L. Pedraz and R. Eritja, Cationic niosomes as non-viral vehicles for nucleic acids: challenges and opportunities in gene delivery, *Pharmaceutics*, 2019, **11**(2), 50.

12 C. Marianecci, L. Di Marzio, F. Rinaldi, C. Celia, D. Paolino, F. Alhaique, S. Esposito and M. Carafa, Niosomes from 80s to present: the state of the art, *Adv. Colloid Interface Sci.*, 2014, **205**, 187–206.

13 M. Schlich, F. Lai, R. Pireddu, E. Pini, G. Ailuno, A. M. Fadda, D. Valenti and C. Sinico, Resveratrol proniosomes as a convenient nanoingredient for functional food, *Food Chem.*, 2020, **310**, 125950.

14 R. Ahmad, S. Srivastava, S. Ghosh and S. K. Khare, Phytochemical delivery through nanocarriers: a review, *Colloids Surf., B*, 2021, **197**, 111389.

15 N. d'Avanzo, M. C. Cristiano, L. Di Marzio, M. C. Bruno, D. Paolino, C. Celia and M. Fresta, Multidrug Idebenone/Naproxen Co-loaded Aspasomes for Significant in vivo Anti-inflammatory Activity, *ChemMedChem*, 2022, **17**(9), e202200067.

16 M. A. Abdelbari, A. A. El-Gazar, A. A. Abdelbary, A. H. Elshafeey and S. Mosallam, Brij integrated bilosomes for improving the transdermal delivery of niflumic acid for effective treatment of osteoarthritis: In vitro characterization, ex vivo permeability assessment, and in vivo study, *Int. J. Pharm.*, 2023, **640**, 123024.

17 A. C. Caritá, J. Resende de Azevedo, Y. Chevalier, D. Arquier, M. V. Buri, K. A. Riske, G. Ricci Leonardi and M. A. Bolzinger, Elastic cationic liposomes for vitamin C delivery: Development, characterization and skin absorption study, *Int. J. Pharm.*, 2023, **638**, 122897.

18 M. A. Altamimi, A. Hussain, W. A. Mahdi, S. S. Imam, M. A. Alshammari, S. Alshehri and M. R. Khan, Mechanistic Insights into Luteolin-Loaded Elastic Liposomes for Transdermal Delivery: HSPiP Predictive Parameters and Instrument-Based Evidence, *ACS Omega*, 2022, **7**(51), 48202–48214.

19 M. B. Marzola Coronel, C. C. Fraenza and E. Anoardo, On the deformability of additivated phosphatidylcholine liposomes: Molecular dynamic regimes and membrane elasticity, *Chem. Phys. Lipids*, 2023, **252**, 105290.

20 D. Paolino, D. Cosco, F. Cilurzo, E. Trapasso, V. M. Morittu, C. Celia and M. Fresta, Improved in vitro and in vivo collagen biosynthesis by asiaticoside-loaded ultradeformable vesicles, *J. Controlled Release*, 2012, **162**(1), 143–151.

21 A. Barone, M. C. Cristiano, F. Cilurzo, M. Locatelli, D. Iannotta, L. Di Marzio, C. Celia and D. Paolino, Ammonium glycyrrhizate skin delivery from ultradeformable liposomes: A novel use as an anti-inflammatory agent in topical drug delivery, *Colloids Surf., B*, 2020, **193**, 111152.

22 R. Muzzalupo and E. Mazzotta, Do niosomes have a place in the field of drug delivery?, *Expert Opin. Drug Delivery*, 2019, **16**(11), 1145–1147.

23 X. Hu, J. Zhang, L. Deng, H. Hu, J. Hu and G. Zheng, Galactose-modified pH-sensitive niosomes for controlled release and hepatocellular carcinoma target delivery of tanshinone IIA, *AAPS PharmSciTech*, 2021, **22**(3), 96.

24 P. Aparajay and A. Dev, Functionalized niosomes as a smart delivery device in cancer and fungal infection, *Eur. J. Pharm. Sci.*, 2022, **168**, 106052.

25 D. Tila, S. N. Yazdani-Arazi, S. Ghanbarzadeh, S. Arami and Z. Pourmoazzen, pH-sensitive, polymer modified, plasma stable niosomes: promising carriers for anti-cancer drugs, *EXCLI J.*, 2015, **14**, 21–32.

26 G. Hao, Z. P. Xu and L. Li, Manipulating extracellular tumour pH: an effective target for cancer therapy, *RSC Adv.*, 2018, **8**, 22182–22192.

27 Y. B. Hu, E. B. Dammer, R. J. Ren and G. Wang, The endosomal-lysosomal system: from acidification and cargo sorting to neurodegeneration, *Transl. Neurodegener.*, 2015, **4**, 18.

28 E. Roux, M. Francis, F. M. Winnik and J. C. Leroux, Polymer based pH-sensitive carriers as a means to improve the cytoplasmic delivery of drugs, *Int. J. Pharm.*, 2002, **242**, 25–36.

29 M. Di Francesco, C. Celia, R. Primavera, N. D'Avanzo, M. Locatelli, M. Fresta, F. Cilurzo, C. A. Ventura, D. Paolino and L. Di Marzio, Physicochemical

characterization of pH-responsive and fusogenic self-assembled non-phospholipid vesicles for a potential multiple targeting therapy, *Int. J. Pharm.*, 2017, **528**, 18–32.

30 S. Sargazi, S. M. Hosseinikhah, F. Zargari, N. P. S. Chauhana, M. Hassanisaadi and S. Amani, pH-responsive cisplatin-loaded niosomes: synthesis, characterization, cytotoxicity study and interaction analyses by simulation methodology, *Nanofabrication*, 2021, **6**, 1–15.

31 F. Marzoli, C. Marianecci, F. Rinaldi, D. Passeri, M. Rossi, P. Minosi, M. Carafa and S. Pieretti, Long-lasting, antinociceptive effects of pH-sensitive niosomes loaded with ibuprofen in acute and chronic models of pain, *Pharmaceutics*, 2019, **11**(2), 62.

32 M. C. Pereira, M. Pianella, D. Wei, A. Moshnikova, C. Marianecci, M. Carafa, O. A. Andreev and Y. K. Reshetnyak, pH-sensitive pHLIP coated niosomes, *Mol. Membr. Biol.*, 2016, **33**, 51–63.

33 M. F. Francis, G. Dhara, F. M. Winnik and J. C. Leroux, In vitro evaluation of pH-sensitive polymer/niosome complexes, *Biomacromolecules*, 2001, **2**, 741–749.

34 W. Zeng, Q. Li, T. Wan, C. Liu, W. Pan, Z. Wu, G. Zhang, J. Pan, M. Qin, Y. Lin, C. Wu and Y. Xu, Hyaluronic acid-coated niosomes facilitate tacrolimus ocular delivery: mucoadhesion, precorneal retention, aqueous humor pharmacokinetics, and transcorneal permeability, *Colloids Surf., B*, 2016, **141**, 28–35.

35 A. Mansoori-Kermani, S. Khalighi, I. Akbarzadeh, F. R. Niavol, H. Motasadizadeh, A. Mahdieh, V. Jahed, M. Abdinezhad, N. Rahbariasr, M. Hosseini, N. Ahmadkhani, B. Panahi, Y. Fatahi, M. Mozafari, A. P. Kumar and E. Mostafavi, Engineered hyaluronic acid-decorated niosomal nanoparticles for controlled and targeted delivery of epirubicin to treat breast cancer, *Mater. Today Bio*, 2022, **16**, 100349.

36 K. Mansouri, S. Rasoulpoor, A. Daneshkhah, S. Abolfathi, N. Salari, M. Mohammadi, S. Rasoulpoor and S. Shabani, Clinical effects of curcumin in enhancing cancer therapy: a systematic review, *BMC Cancer*, 2020, **20**(1), 791.

37 N. G. Vallianou, A. Evangelopoulos, N. Schizas and C. Kazazis, Potential anticancer properties and mechanisms of action of curcumin, *Anticancer Res.*, 2015, **35**(2), 645–651.

38 M. A. Tomeh, R. Hadianamrei and X. Zhao, A review of curcumin and its derivatives as anticancer agents, *Int. J. Mol. Sci.*, 2019, **20**(5), 1033.

39 M. Kharat, G. Zhang and D. J. McClements, Stability of curcumin in oil-in-water emulsions: Impact of emulsifier type and concentration on chemical degradation, *Food Res. Int.*, 2018, **111**, 178–186.

40 M. Urošević, L. Nikolić, I. Gajić, V. Nikolić, A. Dinić and V. Miljković, Curcumin: biological Activities and Modern Pharmaceutical Forms, *Antibiotics*, 2022, **11**(2), 135.

41 R. Tabanelli, S. Brogi and V. Calderone, Improving curcumin bioavailability: current strategies and future perspectives, *Pharmaceutics*, 2021, **13**(10), 1715.

42 P. Anand, A. B. Kunnumakkara, R. A. Newman and B. B. Aggarwal, Bioavailability of curcumin: problems and promises, *Mol. Pharm.*, 2007, **4**(6), 807–818.

43 A. L. Lopresti, The problem of curcumin and its bioavailability: could its gastrointestinal influence contribute to its overall health-enhancing effects?, *Adv. Nutr.*, 2018, **9**(1), 41–50.

44 L. Casula, F. Lai, E. Pini, D. Valenti, C. Sinico, M. C. Cardia, S. Marceddu, G. Ailuno and A. M. Fadda, Pulmonary delivery of curcumin and beclomethasone dipropionate in a multicomponent nanosuspension for the treatment of bronchial asthma, *Pharmaceutics*, 2021, **13**(8), 1300.

45 V. Gugleva, V. Michailova, R. Mihaylova, G. Momekov, M. M. Zaharieva, H. Najdenski, P. Petrov, S. Rangelov, A. Forys, B. Trzebicka and D. Momekova, Formulation and evaluation of hybrid niosomal in situ gel for intravesical co-delivery of curcumin and gentamicin sulfate, *Pharmaceutics*, 2022, **14**(4), 747.

46 D. C. Drummond, M. Zignani and J.-C. Leroux, Current status of pH-sensitive liposomes in drug delivery, *Prog. Lipid Res.*, 2000, **39**(5), 406–460.

47 O. E. Philippova, D. Hourdet, R. Audebert and A. Khokhlov, pH-Responsive Gels of Hydrophobically Modified Poly(acrylic acid), *Macromolecules*, 1997, **30**(26), 8278–8285.

48 X. Xiao, Y. Liu, M. Guo, W. Fei, H. Zheng, R. Zhang, Y. Zhang, Y. Wei, G. Zheng and F. Li, pH-triggered sustained re-lease of arsenic trioxide by polyacrylic acid capped mesoporous silica nanoparticles for solid tumor treatment in vitro and in vivo, *J. Biomater. Appl.*, 2016, **31**, 23–35.

49 S. Saroj and S. J. Rajput, Tailor-made pH-sensitive polyacrylic acid functionalized mesoporous silica nanoparticles for efficient and controlled delivery of anticancer drug etoposide, *Drug Dev. Ind. Pharm.*, 2018, **44**, 1198–1211.

50 A. Hioki, A. Wakasugi, K. Kawano, Y. Hattori and Y. Maitani, Development of an in vitro drug release assay of PEGylated liposome using bovine serum albumin and high temperature, *Biol. Pharm. Bull.*, 2010, **33**(9), 1466–1470.

51 R. Bajoria and S. F. Contractor, Effect of surface charge of small unilamellar liposomes on uptake and transfer of carboxyfluorescein across the perfused human term placenta, *Pediatr. Res.*, 1997, **42**, 520–527.

52 S. Mazumdar, D. Chitkara and A. Mittal, Exploration and insights into the cellular internalization and intracellular fate of amphiphilic polymeric nanocarriers, *Acta Pharm. Sin. B*, 2021, **11**(4), 903–924.

53 M. Nazıroğlu, B. Çiğ, Y. Yazğan, G. K. Schwaerzer, F. Theilig and L. Pecze, Albumin evokes Ca2+-induced cell oxidative stress and apoptosis through TRPM2 channel in renal collecting duct cells reduced by curcumin, *Sci. Rep.*, 2019, **9**, 12403.

54 N. Güllü, J. Smith, P. Herrmann and U. Stein, MACC1-dependent antitumor effect of curcumin in colorectal cancer, *Nutrients*, 2022, **14**(22), 4792.

55 G. Mudduluru, J. N. George-William, S. Muppala, I. A. Asangani, R. Kumarswamy, L. D. Nelson and

H. Allgayer, Curcumin regulates miR-21 expression and inhibits invasion and metastasis in colorectal cancer, *Biosci. Rep.*, 2011, **31**(3), 185–197.

56 L. Zhang, X. Cheng, Y. Gao, C. Zhang, J. Bao, H. Guan, H. Yu, R. Lu, Q. Xu and Y. Sun, Curcumin inhibits metastasis in human papillary thyroid carcinoma BCPAP cells via down-regulation of the TGF-β/Smad2/3 signaling pathway, *Exp. Cell Res.*, 2016, **341**(2), 157–165.

57 Y. Thabet, M. Elsabahy and N. G. Eissa, Methods for preparation of niosomes: a focus on thin-film hydration method, *Methods*, 2022, **199**, 9–15.

58 S. S. D'Souza and P. P. DeLuca, Methods to assess in vitro drug release from injectable polymeric particulate systems, *Pharm. Res.*, 2006, **23**, 460–474.